

Supplement of Geosci. Model Dev., 13, 5119–5145, 2020
<https://doi.org/10.5194/gmd-13-5119-2020-supplement>
© Author(s) 2020. This work is distributed under
the Creative Commons Attribution 4.0 License.



Supplement of

Collisional growth in a particle-based cloud microphysical model: insights from column model simulations using LCM1D (v1.0)

Simon Unterstrasser et al.

Correspondence to: Simon Unterstrasser (simon.unterstrasser@dlr.de)

The copyright of individual parts of the supplement might differ from the CC BY 4.0 License.

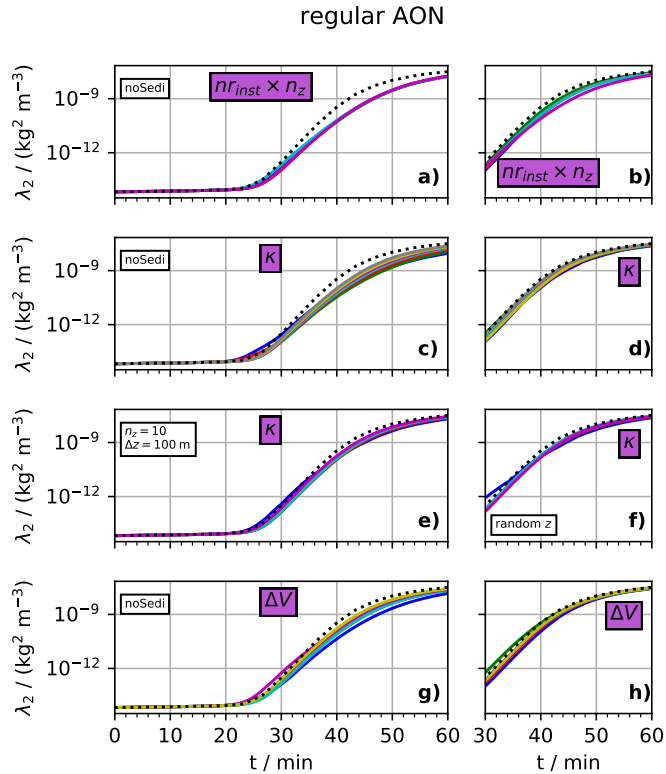


Figure S1. BoxModelEmul set-up: Identical to Fig. 5 in MAIN, except that λ_2 instead of λ_0 is shown.

S1 Introduction

This document contains supplemental material. In the following, MAIN refers to the corresponding GMD paper this supplement belongs to. This document contains additional figures that are not shown in MAIN and also gives an analysis of various limiter implementations which are in particular important in LinSamp-simulations.

5 S2 Box model emulation simulations

In the following, additional plots of the BoxModelEmul simulations, as discussed in section 3.1 of MAIN, are shown.

S2.1 Additional plots for section 3.2.1 "Regular AON version"

Figs. S1 and S2 are identical to Figs. 5 and 6 of MAIN, except that λ_2 instead of λ_0 is shown. Both figures are supposed to demonstrate that convergence in λ_2 is more easily reached than in λ_0 . Hence, MAIN focuses on achieving convergence in

10 terms of λ_0 .

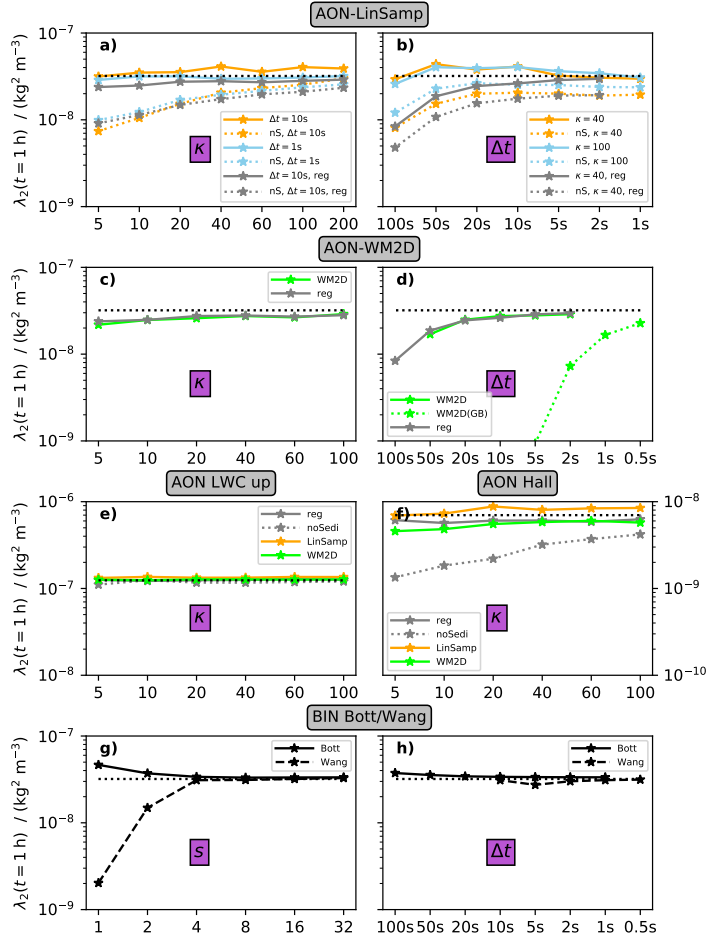


Figure S2. BoxModelEmul set-up: Identical to Fig. 6 in MAIN, except that λ_2 instead of λ_0 is shown. Note that similar to the figure in MAIN, the y -scale ranges over two orders of magnitude.

S2.2 Additional plots for section 3.2.2 "AON version with linear sampling"

In particular for the AON-LinSamp version, the implementation of the limiter is important. The limiter treats cases where $\nu_{\text{coll}} > \max(\nu_i, \nu_j)$. We assume $\nu_j > \nu_i$. The default limiter is given in block LIMITER in Algorithm 1 of MAIN. We tested four different limiter options, which are described in the following.

- 5 – Option LL0: no LIMITER block is included in Algorithm 1 and ν_{coll} is unchanged. Then, SIPs with negative weights are generated. At the end of the time step all SIPs with $\nu_p \leq 0$ are removed. This also destroys mass conservation.
- Option LL1: no LIMITER block is included in Algorithm 1, but in block MULTIPLE COLLECTION we clip ν_{coll} by setting $\nu_{\text{coll}} := \min(\nu_{\text{coll}}, 0.99 \times \nu_j)$.

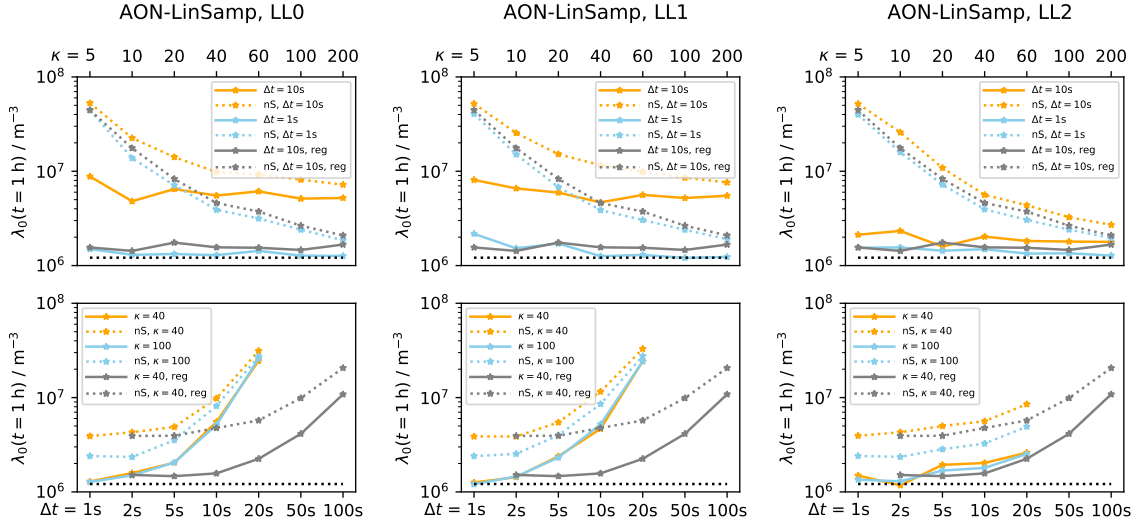


Figure S3. BoxModelEmul set-up: Figure analogous to Fig. 6 of MAIN, now for different limiter implementations as given on top of each column; complements row 1 of Fig. 6 in MAIN. .

- Option LL2: limiter version of Shima et al. (2009). Very similar to our default limiter, but constants 0.5 and 0.5 ("50%,50%"-partitioning) in line 20 of Algorithm 1 instead of 0.6 and 0.4.
- Option LL3: as described in MAIN and Algorithm 1 ("60%,40%"-partitioning)

Figure S3 shows $\lambda_0(t = 1h)$ for the limiter versions LL0, LL1 and LL2. It complements Fig. 6 in MAIN, where the first row shows results for the default limiter LL3. We find that LL2-results are basically identical to LL3 and LL2 and LL3-results are nearly as good as the results of the regular AON (with quadratic sampling). LL0 and LL1 results reveal some deficiencies. Whereas simulations with $\Delta t = 1s$ (blue curves in top row) match well with the regular version (grey curves), the $\Delta t = 10s$ -curves are worse than those of LL2, LL3 and AON-regular.

Consistently, the rower row shows that LL0 and LL1-results get worse with increasing time step, simply due to the fact that limiter cases occur more often.

Figures S4 – S7 show $\lambda(t)$ (plot type is analogous to Fig. 5 of MAIN). Each of the four figures shows results for one particular limiter option as indicated on top of each figure. While LL0 is similar to LL1, and LL2 to LL3, differences between the prior to the letter set become obvious in panels a), e), f), g), and h) How can we interpret that LL0 and LL1 have a similar performance, even though LL0 is supposed to worse by design? Clearly, LL0 "looses" SIPs over time, i.e. N_{SIP} is reduced by 1 when a limiter event occurs. So our interpretation is that a limiter event in LL1 produces a "meaningless" SIP p . "Meaningless" here means that either

- the new values ν_p and μ_p are such that p_{crit} with any other SIP is very low and thus SIP p will not be part in future collection events, or

AON-LinSamp, LL0

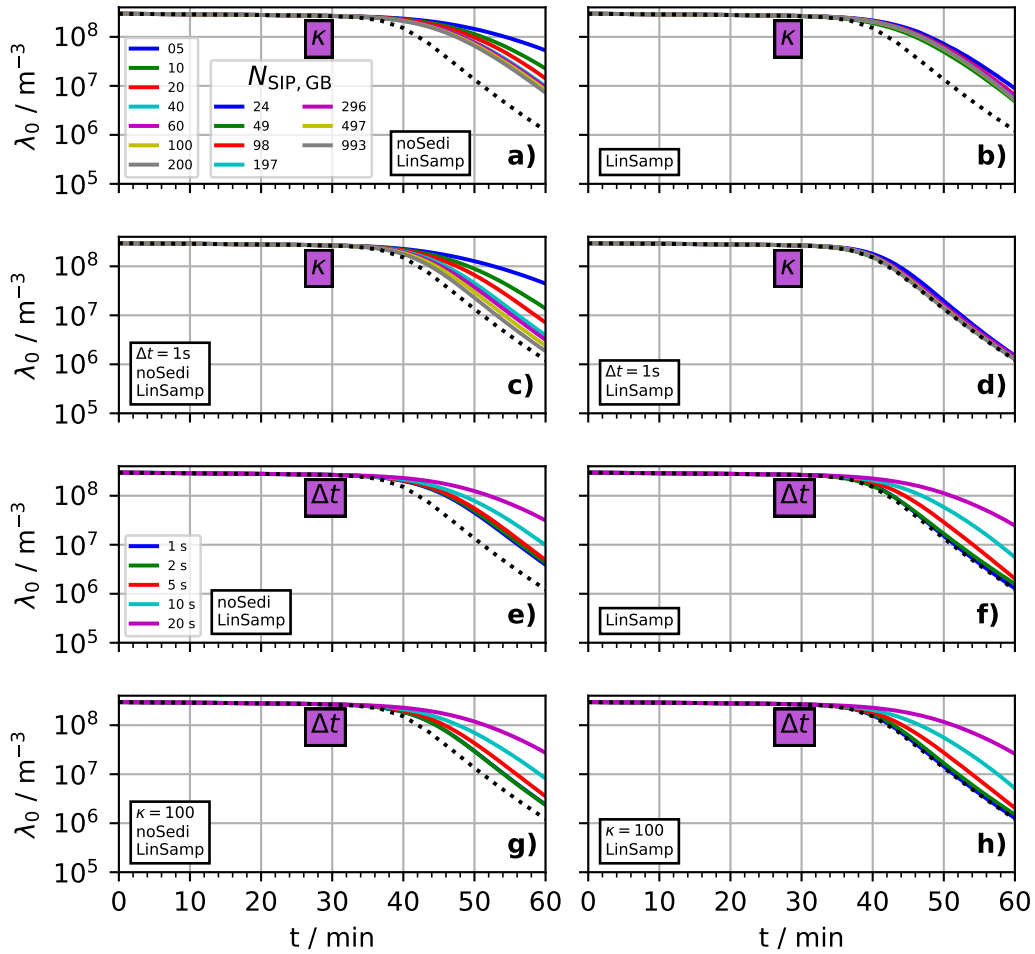


Figure S4. BoxModelEmul set-up: The plots are analogous to Fig. 5 of MAIN (all set-up parameters are listed in that caption), now simulations with linear sampling are depicted (the version of the limiter implementation is given on the top of the plot). The left column shows noSedi simulations, the right column shows full simulations, i.e. with sedimentation..

- ν_p is so small, that even if SIP p is involved in future collections, it has not the potential to change the physical outcome.

AON-LinSamp, LL1

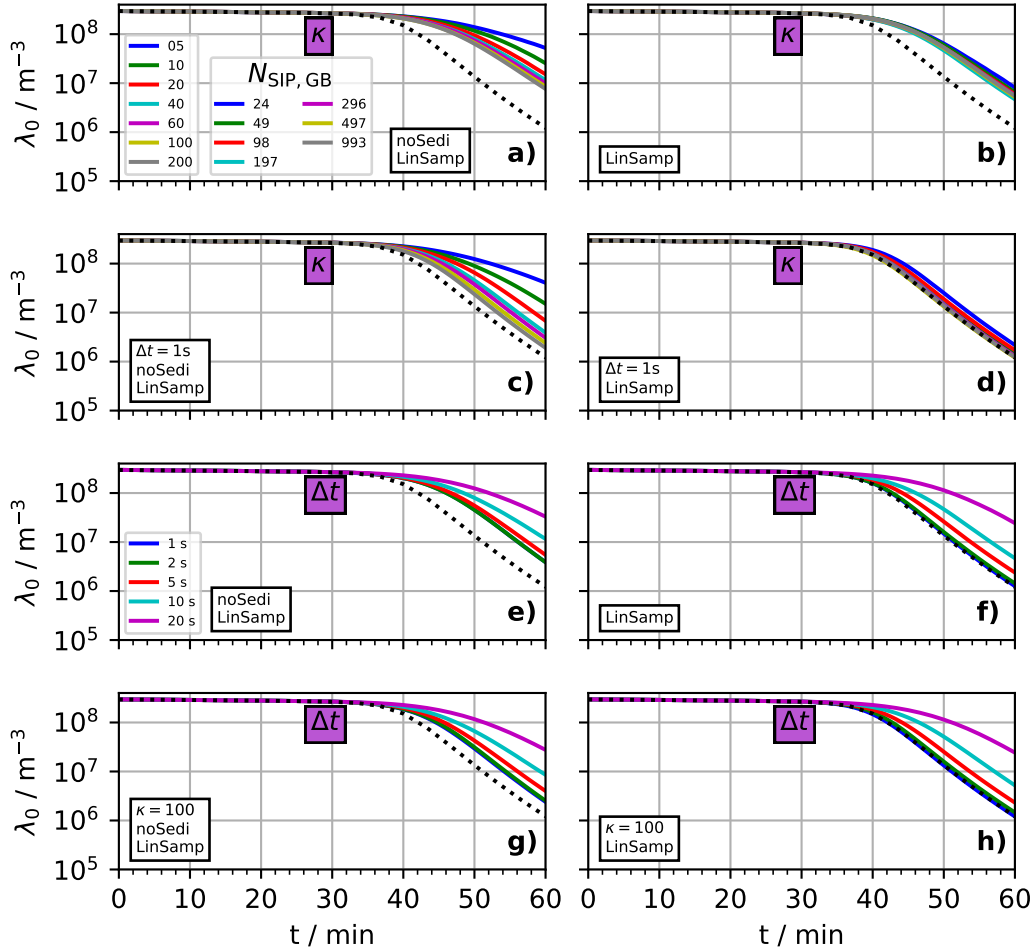


Figure S5. BoxModelEmul set-up: The plots are analogous to Fig. 5 of MAIN (all set-up parameters are listed in that caption), now simulations with linear sampling are depicted (the version of the limiter implementation is given on the top of the plot). The left column shows noSedi simulations, the right column shows full simulations, i.e. with sedimentation..

AON-LinSamp, LL2

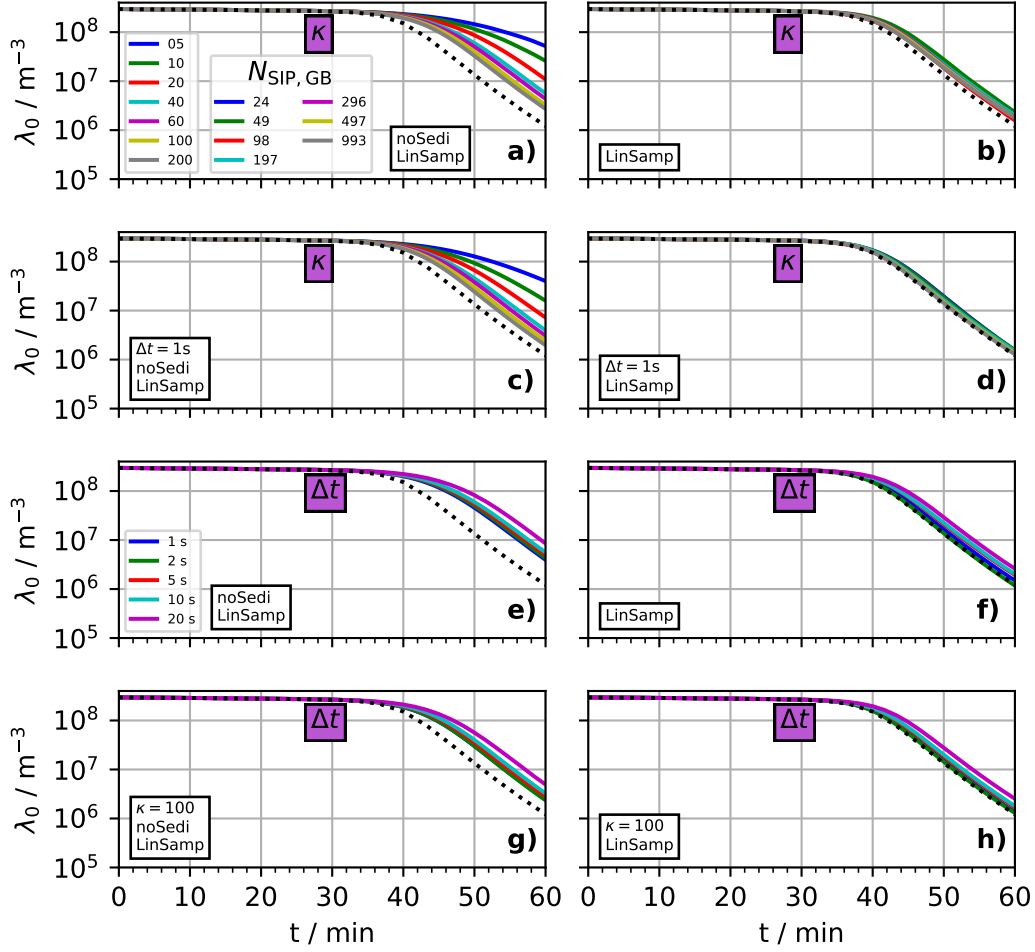


Figure S6. BoxModelEmul set-up: The plots are analogous to Fig. 5 of MAIN (all set-up parameters are listed in that caption), now simulations with linear sampling are depicted (the version of the limiter implementation is given on the top of the plot). The left column shows noSedi simulations, the right column shows full simulations, i.e. with sedimentation..

AON-LinSamp, LL3

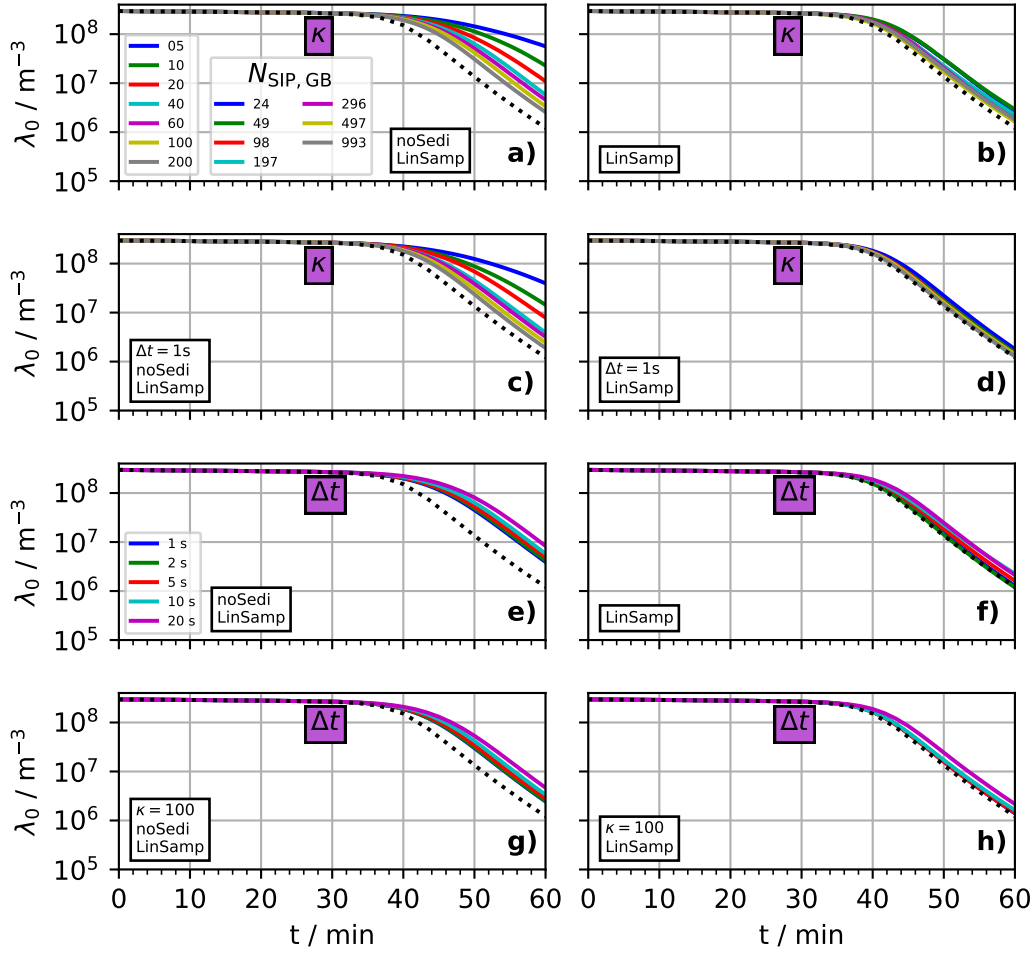


Figure S7. BoxModelEmul set-up: The plots are analogous to Fig. 5 of MAIN (all set-up parameters are listed in that caption), now simulations with linear sampling are depicted (the version of the limiter implementation is given on the top of the plot). The left column shows noSedi simulations, the right column shows full simulations, i.e. with sedimentation..

AON-WM2D

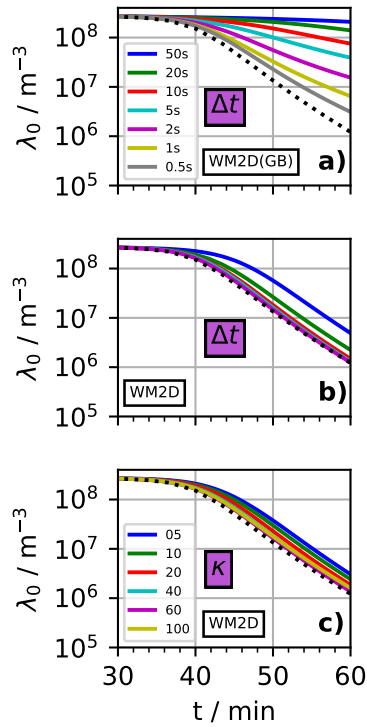


Figure S8. BoxModelEmul set-up: The plot is analogous to Fig. 5 of MAIN (all set-up parameters are listed in that caption), now simulations with explicit overtakes and a 2D well-mixed assumption (as described in section 2.3.2 of MAIN) are depicted. In the top panel overtakes are considered only between SIPs inside the same GB, whereas the other panels show the regular version where overtakes are tested for all SIPs of the column. $\lambda(t = 1 \text{ h})$ of the same simulation set is shown in panels c) and d) of Fig. 6 in MAIN.

S2.3 Additional plots for section 3.2.3 "AON version with explicit overtakes"

Figure S8 shows $\lambda_0(t)$ of AON-WM2D simulations. The same set of simulations is shown in panels c) and d) of Fig. 6 in MAIN.

In the BoxModelEmul set-up, AON-regular and AON-WM2D are supposed to generate identical results (in a statistical sense). Figure S9 demonstrates the statistical equivalence of both AON versions. For this, the mean overtake probability p^{OT} is evaluated in each timestep of an AON-WM2D simulation. In AON-regular, p^{OT} is simply 1. Moreover, the mean p_{crit} is evaluated for each timestep. Clearly, in AON-regular the average is taken over all tested combinations, whereas in AON-WM2D the average is taken over all SIP combinations with an overtake. At the end of section 2.3.2 in MAIN, this average probability p_{crit} was referred to as p^{WM2D} and p^{WM3D} . Finally, the total probabilities are given by $p^{\text{TOT}} = p^{\text{OT}} \times p_{\text{crit}}$. In AON-regular, it

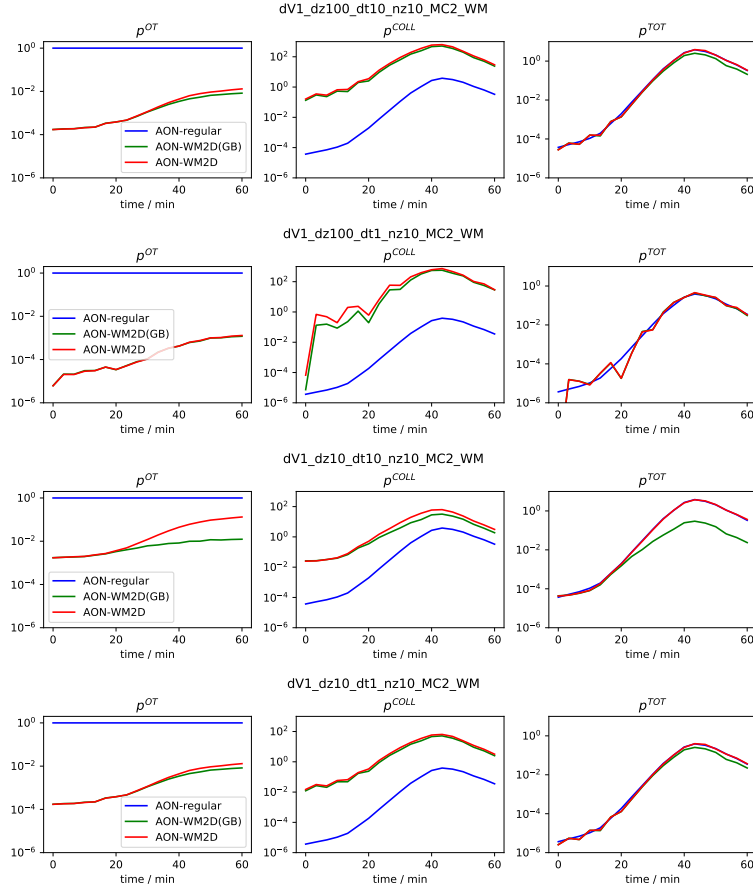


Figure S9. BoxModelEmul set-up: Shows probabilities p^{OT} , p_{crit} , p^{TOT} as defined in section 2.3.2 in MAIN for four different simulations setups and three different AON versions.

is basically much simpler: $p^{\text{TOT}} = p_{\text{crit}} = p^{\text{WM3D}}$. The three columns of figure S9 show the three types of probabilities. Four different sets of simulation parameters are chosen. We vary $\Delta t \in \{1\text{s}, 10\text{s}\}$ and $\Delta z \in \{10\text{m}, 100\text{m}\}$ as they affect p^{OT} . We can see that in all 4 cases p^{TOT} -values of AON-regular and AON-WM2D are the same (blue vs. red curves in third column). Additionally, we add results of the AON-WM2D(GB) where overtakes are considered only between SIPs inside the same GB.

- 5 In the set-up with small Δz and large Δt (third row in figure), many overtakes are missed and p^{OT} of AON-WM2D(GB) is smaller than that of AON-WM2D. Finally, we give a short explanation why the AON-WM2D-curves in the second row are not as smooth as in the other rows. This is simply due to the fact that p^{OT} is very small for this set-up with large Δz and small Δt . Then very few SIP combinations are tested for collection in the second part of the AON-WM2D algorithm.

LWC up

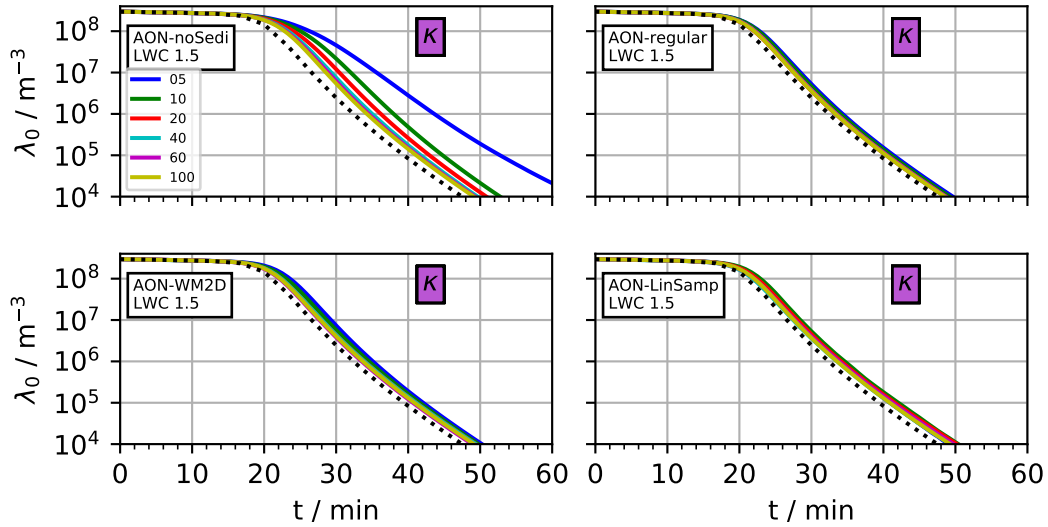


Figure S10. BoxModelEmul set-up: The plot layout is analogous to Fig. 5 of MAIN (all set-up parameters are listed in that caption) and the sensitivity to κ is depicted for simulations with initial $LWC_{\text{init}} = 1.5 \text{ g/m}^3$. The left and right panel juxtapose noSedi and full simulations. $\lambda(t = 1 \text{ h})$ of the same simulation set is shown in panel e) of Fig. 6 in MAIN.

S2.4 Additional plots for section 3.2.4 "Microphysical and bin model sensitivities"

Figure S10 shows $\lambda_0(t)$ of the LWCup simulations as shown in panel e) of Fig. 6 in MAIN.

Figure S11 shows results of the simulation set shown in Fig. 7 of MAIN. The temporal evolution of D_{mean} , λ_0 and λ_2 is shown.

Figure S12 shows $\lambda_0(t)$ of AON simulations with Hall kernel as shown in panel f) of Fig. 6 in MAIN.

- 5 Figure S13 shows $\lambda_0(t)$ of BIN simulations as shown in panels g and h) of Fig. 6 in MAIN.

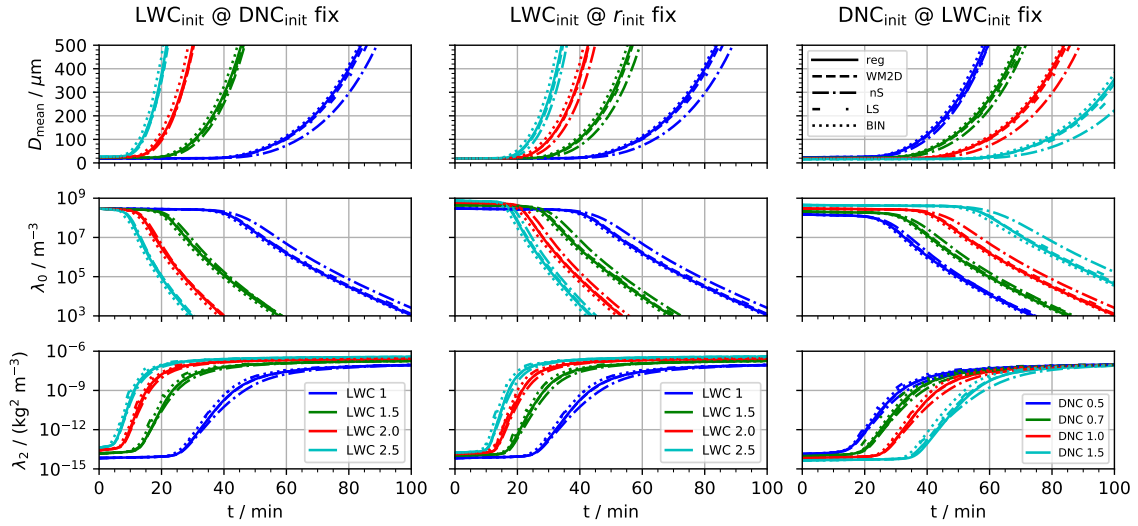


Figure S11. BoxModelEmul set-up: The plot layout is analogous to Fig. 5 of MAIN (all set-up parameters are listed in that caption), now displaying also the temporal evolution of the mean diameter (top row) and the second moment λ_2 (bottom row) additional to λ_0 (middle row). Simulation selection as in Fig. 7 of MAIN. Variations of the initial size distribution parameters LWC_{init} , r_{init} and DNC_{init} are performed. The first and second column show a variation of LWC_{init} (see inserted legend) for either fixed DNC_{init} or r_{init} . The third column shows a DNC_{init} -variation for fixed LWC_{init} . Five different models are used (AON-regular, AON-WM2D, AON-noSedi, AON-LinSamp and BIN; see legend in top right panel).

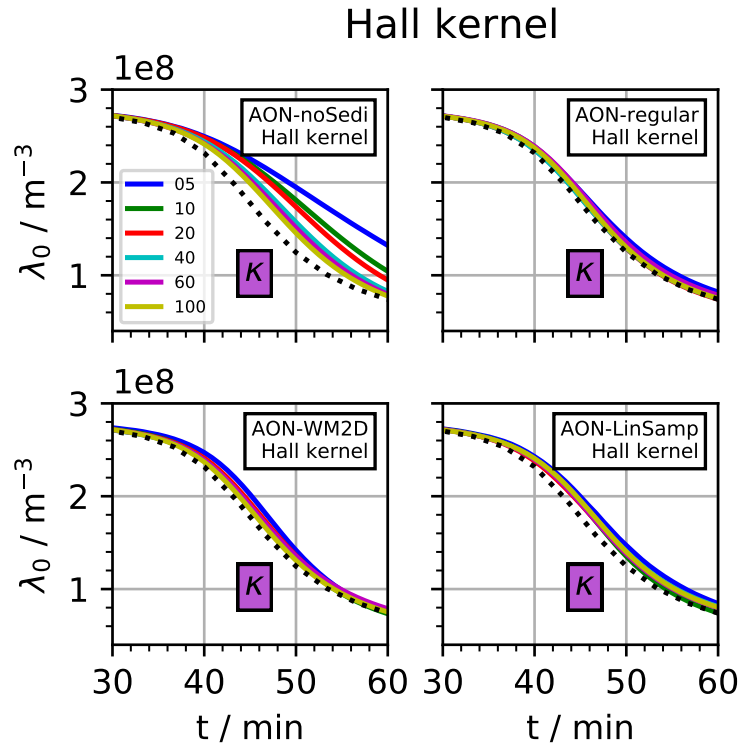


Figure S12. BoxModelEmul set-up: The plot layout is analogous to Fig. 5 of MAIN (all set-up parameters are listed in that caption), now the sensitivity to κ is shown for simulations with the Hall kernel. Each of the four panels shows a different AON version. Unlike to previous plots, the y -axis uses a linear scale. $\lambda(t = 1 \text{ h})$ of the same simulation set is shown in panel f) of Fig. 6 in MAIN.

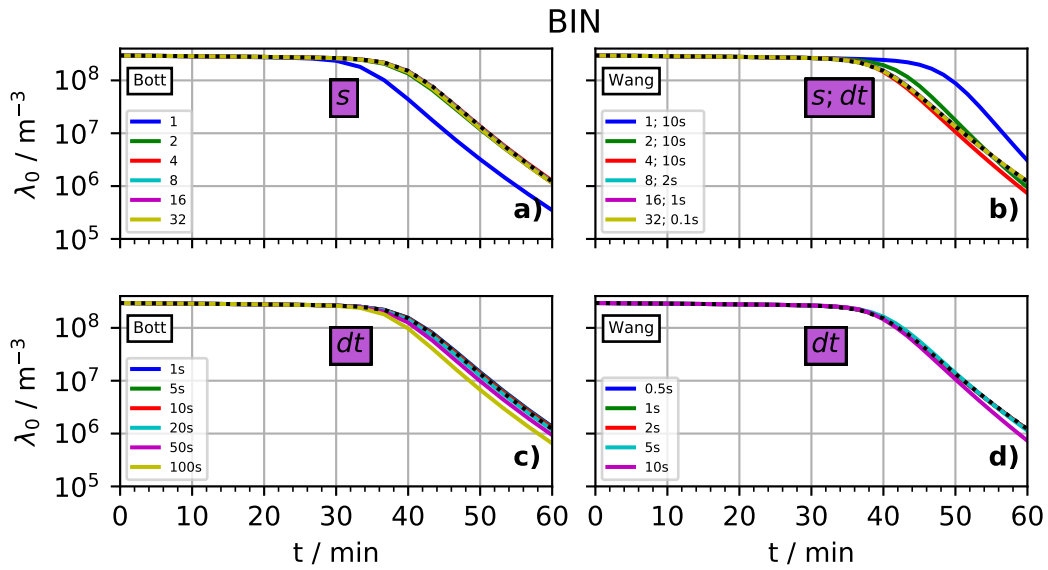


Figure S13. BoxModelEmul set-up: The plot layout is analogous to Fig. 5 of MAIN. The left and right panel juxtapose BIN results with Bott's and Wang's algorithm. were shown . The default parameters are $s = 4$ and $\Delta t = 10s$. Unlike to the AON case, the choice of nz is irrelevant. $\lambda(t = 1 \text{ h})$ of the same simulation set is shown in panels g) and h) of Fig. 6 in MAIN.

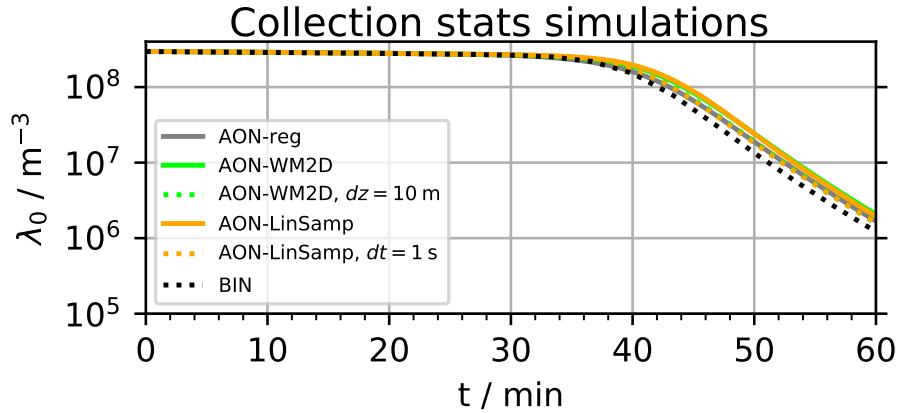


Figure S14. BoxModelEmul set-up: Temporal evolution of column-averaged moment λ_0 over one hour for selected AON versions as in Table 2 and Fig. 8 of MAIN.

S3 Additional plots for section 3.3 "Algorithm Profiling"

Figure S14 shows the temporal evolution of λ_0 and demonstrates convergence for the selected AON simulations. The same selection of simulations was chosen in Table 2 and Fig. 8 of MAIN.

In the following, the right-most column of Fig. 8 of MAIN is reproduced using other limiter implementations. Table 2 of
5 MAIN shows collection statistics for two LinSamp simulations (block #4 & #5). Table S1 of SUPP shows the corresponding blocks for all four limiter implementations. Note that in LL0 no actual limiter is employed and N_{LI} counts the removals of negative weight SIPs. For AON-LinSamp, the number of tested combinations is constant over time and should be the same for the various limiter implementations. Only for LL0, we find N_{comb} to decrease as the SIP number decreases over time. N_{LI} is higher in LL0 and LL1 than in LL2 and LL3. The number of the fractions $\eta_{OT}, \eta_{NO}, \eta_{SI}$ and η_{MU} of LL1, LL2 and LL3 do
10 not differ much. Figure S16 demonstrates that all four limiter implementations produce basically identical results, at least for the two time steps used here ($\Delta t = 1$ s or 5 s). Indeed, the bottom row of Fig. S3 shows that LL0 and LL1-results get worse only for $\Delta t \geq 10$ s. This shows that for the current set-up astonishingly many limiter cases can occur ($N_{LI} = 1528$ in LL1) and the simulation results are still acceptable. We find that limiter events are more numerous in LL1 than in LL2 and LL3 (by a factor of 15). This adds another interpretation for the LL1-failure. Apparently, the limiter operation in LL1 produces SIPs that
15 subsequently trigger limiter events and favors a cascade of limiter events.

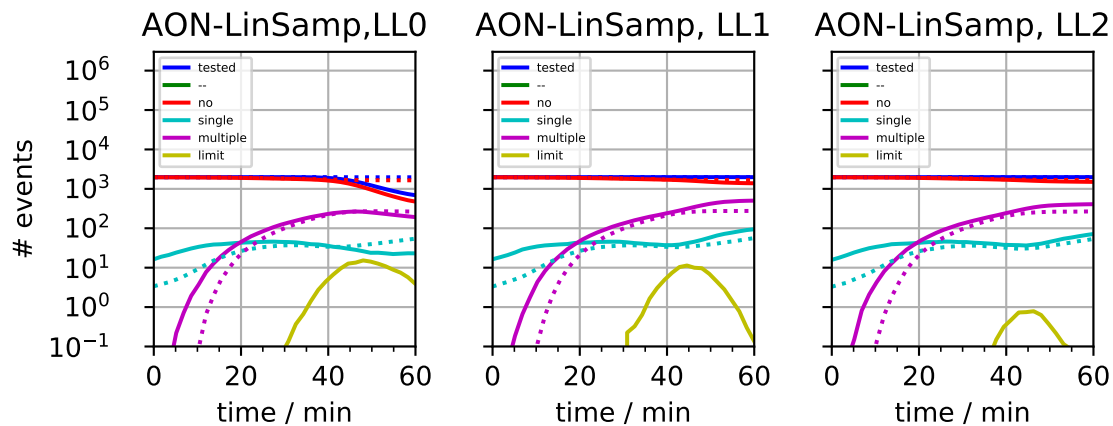


Figure S15. BoxModelEmul set-up: Analogous to Fig 8 of MAIN, here for different limiter implementations (as given on top of each panel). In MAIN, the right-most panel of Fig. 8 shows LinSamp version LL3, which is left out here. The solid curves show simulations with $\Delta t = 5$ s, whereas the dotted curves show the $\Delta t = 1$ s-simulation.

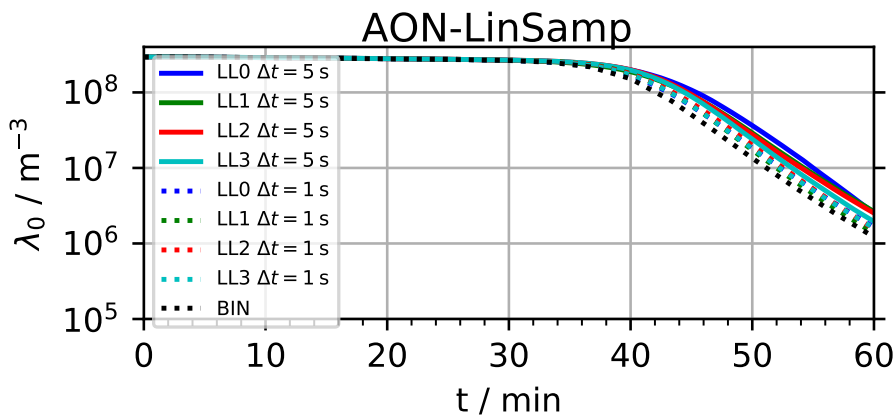


Figure S16. BoxModelEmul set-up: Temporal evolution of column-averaged moment λ_0 over one hour for all LinSamp versions as used Table S1 and Figs.

Table S1. BoxModelEmul set-up: Analogous to Table 2 of MAIN , now showing various limiter implementations for AON-LinSamp. The default time step is $\Delta t = 5$ s.

Limiter implementation	tested SIP combinations	overtakes	no collection	single collection	multiple collection	limiter event	$\sum p_{\text{crit}}$	\bar{p}_{crit}
AON-LinSamp	N_{comb}	η_{OT}	η_{NO}	η_{SI}	η_{MU}	N_{LI}		
LL0	4.76e5	-	98.0%	1.6%	0.5%	0	3.08e4	6.48e-2
	4.73e5	-	91.1%	2.2%	6.8%	196	3.66e7	7.74e1
	2.93e5	-	78.5%	2.1%	19.3%	2427	5.58e8	1.90e3
	1.24e6	-	90.7%	1.9%	7.3%	2624	5.95e8	4.79e2
LL0, $\Delta t = 1$ s	2.38e6	-	99.3%	0.5%	0.1%	0	3.16e4	1.33e-2
	2.38e6	-	92.8%	1.7%	5.4%	0	4.43e7	1.86e1
	2.36e6	-	84.6%	2.1%	13.3%	33	2.02e8	8.54e1
	7.12e6	-	92.3%	1.5%	6.3%	33	2.46e8	3.46e1
LL1	4.76e5	-	97.9%	1.6%	0.5%	0	3.01e4	6.33e-2
	4.76e5	-	91.0%	2.1%	6.9%	215	3.36e7	7.06e1
	4.76e5	-	76.3%	3.2%	20.5%	1313	3.21e8	6.74e2
	1.43e6	-	88.4%	2.3%	9.3%	1528	3.54e8	2.48e2
LL1, $\Delta t = 1$ s	2.38e6	-	99.3%	0.5%	0.1%	0	3.08e4	1.30e-2
	2.38e6	-	93.0%	1.7%	5.3%	0	4.13e7	1.74e1
	2.38e6	-	84.5%	2.1%	13.4%	6	1.84e8	7.73e1
	7.14e6	-	92.3%	1.5%	6.3%	6	2.25e8	3.15e1
LL2	4.76e5	-	98.0%	1.6%	0.5%	0	3.04e4	6.39e-2
	4.76e5	-	91.0%	2.2%	6.8%	11	3.78e7	7.95e1
	4.76e5	-	79.3%	2.5%	18.2%	84	3.11e8	6.54e2
	1.43e6	-	89.4%	2.1%	8.5%	95	3.49e8	2.45e2
LL2, $\Delta t = 1$ s	2.38e6	-	99.3%	0.5%	0.1%	0	3.07e4	1.29e-2
	2.38e6	-	93.2%	1.7%	5.1%	0.30	4.08e7	1.72e1
	2.38e6	-	85.2%	1.9%	12.8%	0.50	1.91e8	8.01e1
	7.14e6	-	92.6%	1.4%	6.0%	0.80	2.32e8	3.24e1
LL3	4.76e5	-	97.9%	1.6%	0.5%	0	2.95e4	6.20e-2
	4.76e5	-	90.9%	2.2%	6.9%	11	3.59e7	7.55e1
	4.76e5	-	78.7%	2.6%	18.7%	87	2.55e8	5.35e2
	1.43e6	-	89.2%	2.1%	8.7%	99	2.91e8	2.04e2
LL3, $\Delta t = 1$ s	2.38e6	-	99.3%	0.6%	0.1%	0	3.34e4	1.41e-2
	2.38e6	-	92.9%	1.7%	5.4%	0	4.39e7	1.84e1
	2.38e6	-	85.0%	2.0%	12.9%	0.40	1.95e8	8.20e1
	7.14e6	-	92.4%	1.4%	6.2%	0.40	2.39e8	3.35e1

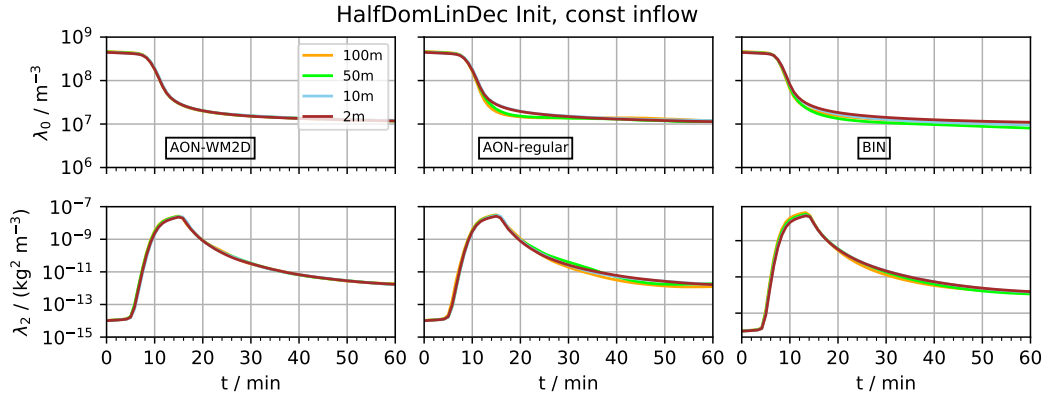


Figure S17. HalfDomLinDec set-up: Temporal evolution of column-averaged moments λ_0 and λ_2 for various model versions (from left to right: AON-WM2D, AON-regular, BIN). Each panel shows a variation of the vertical resolution Δz (see legend). In LCM simulations, SIP numbers for $\Delta z = 100\text{m}$ and 50m -simulations are increased to the level of the $\Delta z = 10\text{m}$ -simulation.

S4 Realistic column model simulations

S4.1 Additional plots for section 3.4.1 "Half domain set-up"

Figure S17 demonstrates that in the **HalfDomLinDec** simulations a variation of Δz has virtually no impact on the results. The implications of this are discussed in MAIN.

- 5 Fig. S18 presents various BIN simulations with different timesteps Δt and r_{CFL} . Both parameter in combination determine the local CFL number of each bin. Obviously, these variations have no impact on the physical outcome of the BIN simulations.

S4.2 Additional plots for section 3.4.2 "Empty domain set-up"

Figure S19 is an extension of Fig. 14 in MAIN, as the present plot additionally shows λ_2 .

- 10 Figure S20 demonstrates that the differences between $\Delta z = 100\text{m}$ and $\Delta z = 10\text{m}$ remain across many AON-WM3D simulations. For $\Delta z = 100\text{m}$ and $\Delta z = 10\text{m}$, Figure S20 shows the *DNC*-evolution of AON-WM3D simulations with different parameter settings. The green curves show the default case from before, where the $\Delta z = 100\text{m}$ -simulation uses a "10x" higher $N_{\text{SIP,GB}}$ -value. We used LinSamp instead of QuadSamp (red), further decreased the time step from $\Delta t = 10\text{s}$ to 1s (blue) or used for both resolutions the same $N_{\text{SIP,GB}}$ -value (which reduces $N_{\text{SIP,tot}}$ of the $\Delta z = 100\text{m}$ -simulation by a factor of ten; orange). In all cases, the Δz -dependence appears consistently.

- 15 Moreover, Figure S21 demonstrates that the DSD that is made up of all SIPs leaving the lower domain boundary is not much affected by the choice of Δz .

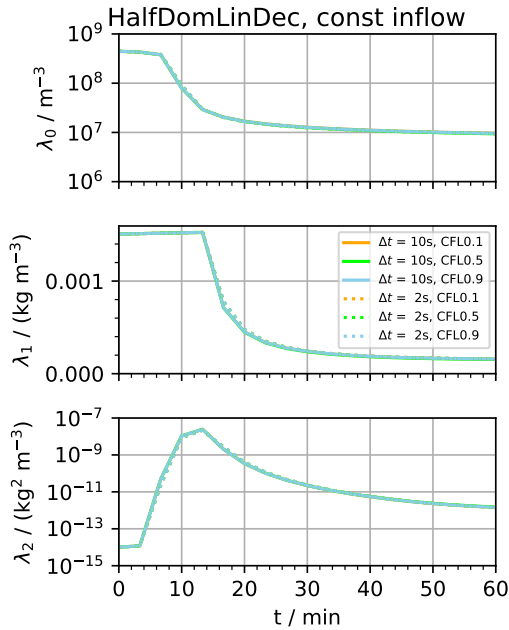


Figure S18. HalfDomLinDec set-up: Temporal evolution of column-averaged moments λ_0 , λ_0 and λ_2 for various BIN simulations. The default BIN parameter settings are: maximum CFL number $r_{\text{CFL}} = 0.5$ and $\Delta t = 10\text{s}$. This plot also shows results for $\Delta t = 2\text{s}$ and maximum CFL numbers of 0.1 and 0.9.

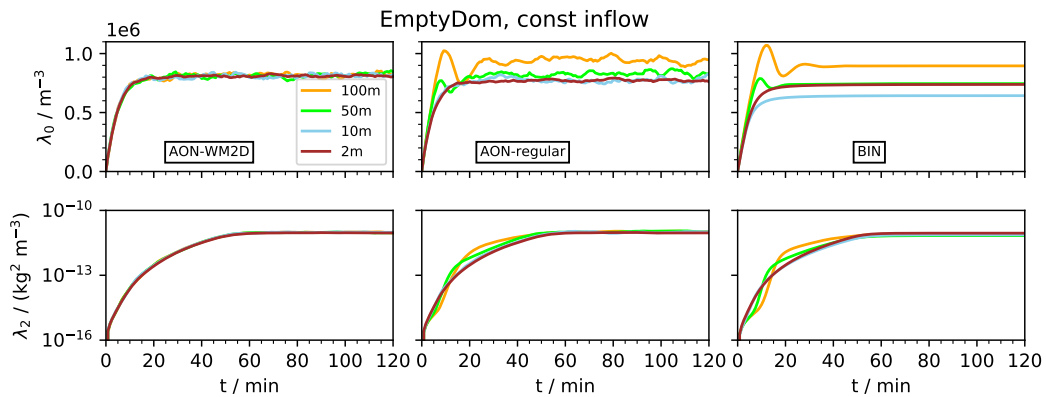


Figure S19. EmptyDom set-up: Temporal evolution of column-averaged moment λ_0 for various model versions (from left to right: AON-WM2D, AON-regular, BIN). Each panel shows a variation of the vertical resolution Δz (see legend). In LCM simulations, SIP numbers for $\Delta z = 100\text{m}$ and 50m -simulations are increased to the level of the $\Delta z = 10\text{m}$ -simulation.

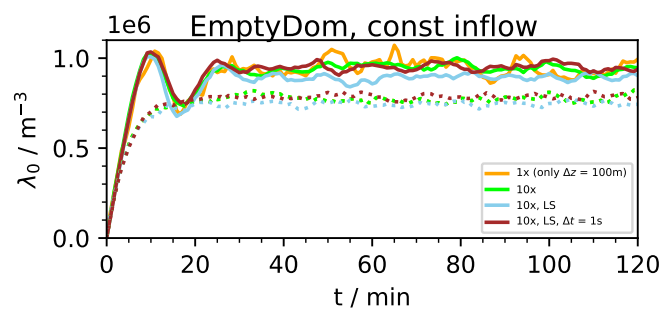


Figure S20. EmptyDom set-up: Temporal evolution of column-averaged moments λ_0 and λ_2 for the AON-WM3D model. Results for various parameter settings (see legend) are depicted for $\Delta z = 100\text{ m}$ (solid) and $\Delta z = 10\text{ m}$ (dotted).

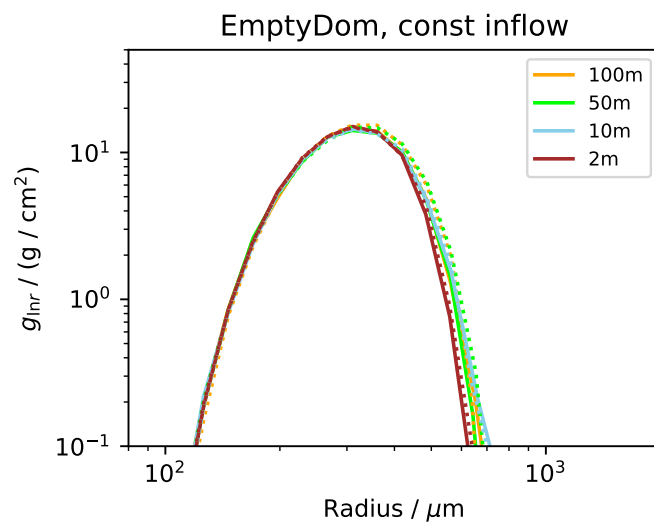


Figure S21. EmptyDom set-up: Size distribution of all droplets that crossed the lower boundary. AON-WM3D (dotted) and AON-WM2D (solid) results for various vertical resolutions Δz are displayed (see inserted legend for the colour coding).

References

- S. Shima, K. Kusano, A. Kawano, T. Sugiyama, and S. Kawahara. The super-droplet method for the numerical simulation of clouds and precipitation: a particle-based and probabilistic microphysics model coupled with a non-hydrostatic model. *Q. J. R. Meteorol. Soc.*, 135 (642):1307–1320, 2009. <https://doi.org/10.1002/qj.441>.